

LA-UR- 02-6319

Approved for public release;
distribution is unlimited.

Title: Modeling Pollutant Transport using a Meshless-Lagrangian Particle Model

Author(s): David Bradley Carrington - LANL, CCS-4
Darrell W. Pepper - University of Nevada, Las Vegas

Submitted to: SIAM - Geosciences Conference
to be held in March 2003 at
Austin, Texas



Los Alamos National Laboratory, an affirmative action/equal opportunity employer, is operated by the University of California for the U.S. Department of Energy under contract W-7405-ENG-36. By acceptance of this article, the publisher recognizes that the U.S. Government retains a nonexclusive, royalty-free license to publish or reproduce the published form of this contribution to allow others to do so, for U.S. Government purposes. Los Alamos National Laboratory requests that the publisher identify this article as work performed under the auspices of the U.S. Department of Energy. Los Alamos National Laboratory strongly supports academic freedom and a researcher's right to publish; as an institution, however, the Laboratory does not endorse the viewpoint of a publication or guarantee its technical correctness.

Form 836 (8/00)

Modeling Pollutant Transport using a Meshless-Lagrangian Particle Model

David B. CARRINGTON* and Darrell W. PEPPER**

*Los Alamos National Laboratory,

**College of Engineering, University of Nevada Las Vegas, Las Vegas, NV 89154-4027

keywords: atmospheric dispersion, finite element, meshless, particle transport, random walk

Extended Abstract

Overview

A combined meshless-Lagrangian particle transport model is used to predict pollutant transport over irregular terrain. The numerical model for initializing the velocity field is based on a meshless approach utilizing multiquadrics established by Kansa. The Lagrangian particle transport technique uses a random walk procedure to depict the advection and dispersion of pollutants over any type of surface, including street and city canyons.

Introduction

An enormous amount of effort has been devoted to the development of efficient algorithms for the numerical solution of partial differential equations. For decades, the finite element method (FEM) and the finite difference/finite volume methods (FDM/FVM) have been the dominant numerical schemes employed in most scientific computation. These methods have been used to solve technical problems from aircraft and auto design to medical imaging. Even so, there are often substantial difficulties in applying these techniques, particularly for complicated domain and/or three-dimensional problems. A common difficulty in the FEM and the FDM/FVM is the considerable amount of time and effort required to discretize and index the domain elements. This is often the most time consuming part of the solution process and is far from being fully automated, particularly in 3D. One method for alleviating this difficulty is to use the boundary element method (BEM). The major advantage of the BEM is that only boundary discretization is required rather than domain. Efficiency is significantly improved over these more traditional methods. However, the BEM involves sophisticated mathematics beyond the FEM and FDM/FVM and some difficult numerical integration of singular functions. Furthermore, the discretization of surfaces in 3-D can still be a complex process even for simple shapes. In addition, all these traditional methods are often slowly convergent, frequently requiring the solution of 10's-100's of thousands of equations in order to get acceptable accuracy.

In recent years, a novel numerical technique called "meshless methods" (or "mesh-free methods") has been undergoing strong development and has attracted considerable attention from both science and engineering communities. Currently, meshless methods now being developed in many research institutions all over the world.

A common feature of meshless methods is that neither domain nor surface meshing is required during the solution process. These methods are designed to handle problems with large deformation, moving boundaries, and complicated geometry. Recently, advances in the development and application of meshless techniques show they can be strong competitors to the more classical finite difference/volume and finite element approaches [1, 2]. Indeed, research in meshless methods has continued to grow at a rapid pace over the past few years. It is expected that meshless methods will become a dominant numerical method for solving science and engineering problems in the 21st century.

A recent book by Liu [3] discusses meshfree methods, implementation, algorithms, and coding issues for stress-strain problems, and includes Mfree2D, an adaptive stress analysis software package available for free from the web [4]. Atluri and Shen [5] also recently produced a research monograph that describes the meshless method in detail, including much in-depth mathematical basis.

The Meshless Method using RBFs

Various types of meshless methods exist with each method having its advantages and disadvantages. Intensive research conducted in many major research institutions all over the world are now working to improve the performance of these approaches. In this work, we focus on the use of radial basis functions (RBFs) – which are simple to implement. Currently, there are two major approaches in this direction: (i) a domain-type meshless method that was developed by Kansa [6] in 1990; (ii) a boundary-type meshless method that has evolved from the BEM.

Radial basis functions are the natural generalization of univariate polynomial splines to a multivariate setting. The main advantage of this type of approximation is that it works for arbitrary geometry with high dimensions and it does not require a mesh at all. A RBF is a function whose value depends only on the distance from some center point. Using distance functions, RBFs can be easily implemented to reconstruct a plane or surface using scattered data in 2-D, 3-D or higher dimensional spaces.

From the theory of radial basis functions, the given function is approximated by a linear combination of radial functions centered in points scattered throughout the domain of interest; i.e.,

$$f(x) \approx s(x) = \sum_{j=1}^N c_j \phi(|x - x_j|), \quad x \in \Omega, \quad (1)$$

where $\{c_1, c_2, \dots, c_j\}$ is the unknown coefficient to be determined, ϕ the trial function and $|\bullet|$ the Euclidean distance. For convenience, we denote $r = |\bullet|$. Some popular choices of trial function ϕ include linear (r), cubic (r^3), multiquadrics (MQ) ($(r^2 + c^2)^{1/2}$), polyharmonic splines ($r^{2n+1} \log r$ in 2-D, r^{2n+1} in 3-D), and Gaussian ($\exp(-cr^2)$). The unknown coefficients can be computed by a collocation method, which means the $s(x)$ reproduces the original given data set; i.e.,

$$f(x_i) = s(x_i) = \sum_{j=1}^N c_j \phi(|x_i - x_j|), \quad i = 1, 2, \dots, N. \quad (2)$$

The above expression implies a linear system whose size is equal to the number of scattered data points. Once the unknown coefficients are obtained by solving above linear system of equations, one can approximate $f(x)$ by $s(x)$ at any point x in Ω . For further details, we refer readers to the theory of RBFs discussed in Powell [7].

In 1990, Kansa [6] extended the idea of interpolation scheme using RBFs to solving various types of engineering problems. The method is simple and direct and is becoming very popular in the engineering community. The boundary type meshless methods indicated in the last section is rather technical and we will only focus on a brief introduction of Kansa's method in this section.

To illustrate the application of the meshless method using Kansa's method, we first consider the elliptic problems. For simplicity, we consider the 2D Poisson problem with Dirichlet boundary condition

$$\begin{aligned} \nabla^2 T &= f(x, y), \quad (x, y) \in \Omega, \\ T &= g(x, y), \quad (x, y) \in \Gamma. \end{aligned} \quad (3)$$

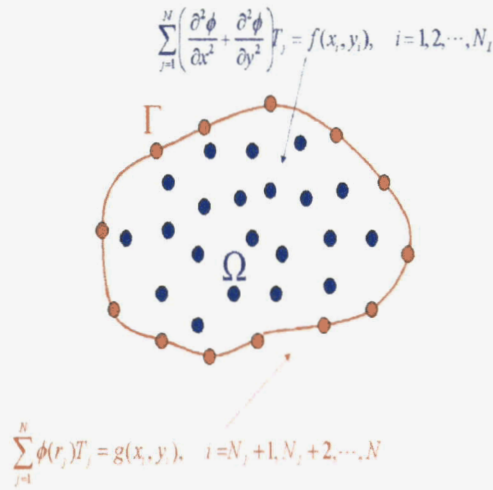


Figure 1. Interior points and boundary points using Kansa's method.

For time dependent problems, we consider the following heat equation as an example:

$$\frac{\partial T}{\partial t} - \alpha \nabla^2 T = f(x, y, T, \frac{\partial T}{\partial x}, \frac{\partial T}{\partial y}) \quad (9)$$

An implicit time marching scheme can be used and (9) becomes

$$\frac{T^{n+1} - T^n}{\Delta t} - \alpha \left(\frac{\partial^2 T^{n+1}}{\partial x^2} + \frac{\partial^2 T^{n+1}}{\partial y^2} \right) = f(x, y, T^n, \frac{\partial T^n}{\partial x}, \frac{\partial T^n}{\partial y}) \quad (10)$$

where Δt denotes the time step and superscript $n+1$ is the unknown (or next time step) value to be solved and superscript n is the current known value. The approximate solution can be expressed as

$$\hat{T}(x, y, t^{n+1}) = \sum_{j=1}^N T_j^{n+1} \phi_j(x, y) \quad (11)$$

Substituting Eq. (11) into Eq. (10), one obtains

$$\begin{aligned} & \sum_{j=1}^N T_j^{n+1} \left(\frac{\phi_j}{\Delta t} - \alpha \left(\frac{\partial^2 \phi}{\partial x^2} + \frac{\partial^2 \phi}{\partial y^2} \right) \right) (x_i, y_i) = \\ & \frac{1}{\Delta t} T^n(x_i, y_i) + f(x_i, y_i, t^n, T^n(x_i, y_i), T_x^n(x_i, y_i), T_y^n(x_i, y_i)) \quad i = 1, 2, \dots, N_i \\ & \sum_{j=1}^N T_j^{n+1} \phi(x_i, y_i) = g(x_i, y_i, t^{n+1}) \quad i = N_i + 1, \dots, N \end{aligned} \quad (12)$$

which produces an $N \times N$ linear system of equations for the unknown T_j^{n+1} . Note that the right hand side of the first equation in Eq. (12) can be updated before the next time step is proceed as follows:

$$T^n(x_i, y_i) = \sum_{j=1}^N T_j^n \phi_j(x_i, y_i), \quad T_x^n(x_i, y_i) = \sum_{j=1}^N T_j^n \frac{\partial \phi_j}{\partial x}(x_i, y_i), \quad T_y^n(x_i, y_i) = \sum_{j=1}^N T_j^n \frac{\partial \phi_j}{\partial y}(x_i, y_i). \quad (13)$$

Notice that the solution of Eq. (3) is in fact nothing but a surface. The technique in surface interpolation shown in the last section can be applied to solve Eq. (3). To approximate T , Kansa [6] proposed to assume the approximate solution can be approximated by a linear combination of RBFs

$$\hat{T}(x, y) = \sum_{j=1}^N T_j \phi(r_j) \quad (4)$$

where $\{T_1, T_2, \dots, T_N\}$ are the unknown coefficients to be determined, $\phi(r_j)$ is some form of RBF (trial function), and r is defined as

$$r_j = \sqrt{(x - x_j)^2 + (y - y_j)^2}. \quad (5)$$

Since MQ is an infinitely smooth function, it is often chosen as the trial function for ϕ , i.e.,

$$\phi(r_j) = \sqrt{r_j^2 + c^2} = \sqrt{(x - x_j)^2 + (y - y_j)^2 + c^2} \quad (6)$$

where c is a shape parameter provided by the user. The optimal value of c is still a subject of outstanding research. We will not further elaborate it here. Other trial function such as polyharmonic splines can also be chosen as the trial function.

By direct differentiation of Eq. (6), the first and second derivatives of ϕ with respect to x and y can be expressed as

$$\begin{aligned} \frac{\partial \phi}{\partial x} &= \frac{x - x_j}{\sqrt{r_j^2 + c^2}}, & \frac{\partial \phi}{\partial y} &= \frac{y - y_j}{\sqrt{r_j^2 + c^2}} \\ \frac{\partial^2 \phi}{\partial x^2} &= \frac{(y - y_j)^2 + c^2}{\sqrt{r_j^2 + c^2}^3}, & \frac{\partial^2 \phi}{\partial y^2} &= \frac{(x - x_j)^2 + c^2}{\sqrt{r_j^2 + c^2}^3} \end{aligned} \quad (7)$$

Substituting (7) into (1) and by collocation method, one obtains

$$\begin{aligned} \sum_{j=1}^N T_j \left(\frac{(x_i - x_j)^2 + (y_i - y_j)^2 + 2c^2}{((x_i - x_j)^2 + (y_i - y_j)^2 + c^2)^{3/2}} \right) &= f(x_i, y_i), \quad i = 1, 2, \dots, N_I \\ \sum_{j=1}^N T_j \sqrt{(x_i - x_j)^2 + (y_i - y_j)^2 + c^2} &= g(x_i, y_i), \quad i = N_I + 1, N_I + 2, \dots, N \end{aligned} \quad (8)$$

where N_I denotes the total number of interior points and $N_I + 1, \dots, N$ are the boundary points. Figure 1 shows two sets of interpolation points: interior and boundary points. Note that Eq. (8) is a linear system of $N \times N$ equations and can be solved by direct Gaussian elimination. Once the unknown coefficients $\{T_1, T_2, \dots, T_N\}$ are found, the solution of T in (3) can be approximated by (4) at any point in the domain.

Meshless Method for Pollutant Transport

Successful prediction of hazardous material trajectories requires accuracy in depicting the wind field. Past efforts have been spent in examining various numerical methods for simulating atmospheric flows, especially those methods that automatically maintain dispersion error control [8, 9]. Recent and accurate scheme that is capable of dealing with highly irregular terrain including city buildings is the meshless method.

Meshless Method for Diagnostic Analysis

Meteorological data obtained from observations and tower measurements help create a 3-D wind field over complex terrain. Surface wind fields are constructed from the meteorological tower data and interpolated to the initial node points using the meshless method. The method uses the tower data points as nodes from which to interpolate. The process utilizes a collocation method as given by

$$\sum_{i=1}^n a_i \frac{r^2 + 2c^2}{(r^2 + c^2)^3} = f(x_j, y_j, z_j) \quad (14)$$

where

$$r = \|x - x_i\| \quad (15)$$

and c is a free parameter dependent on the domain, usually between 0.2 and 2.

For example, the function $f(x, y) = \nabla^2 u$ in 2-D is discretized as

$$f(x, y) = \sum_{i=1}^n a_i \frac{(x - x_i)^2 + c^2}{\left(\sqrt{(x - x_i)^2 + (y - y_i)^2 + c^2}\right)^3} + \sum_{i=1}^n a_i \frac{(y - y_i)^2 + c^2}{\left(\sqrt{(x - x_i)^2 + (y - y_i)^2 + c^2}\right)^3} \quad (16)$$

Solving the resultant linear system of equations, we obtain $\{a_i\}$. With the coefficients ' a_i ' known, values for ' u ' can be obtained from

$$u = \sum_{i=1}^n a_i \sqrt{r^2 + c^2} \quad (17)$$

at any point in the domain [6].

A weighting of r^{-1} is used for the upper level velocity and temperature measurements. This weighting produces a smooth field, as opposed to r^{-2} weighting. Mixing depth is also interpolated using the r^{-1} procedure. Once the surface level flow field has been established and the upper level wind data interpolated, the horizontal divergence is removed with an iterative process. A final refinement using an Euler-Lagrange optimization, which is subject to mass continuity, reduces the remaining divergence globally over the entire 3-D domain [8, 9].

Lagrangian Particle Transport

For point sources, Lagrangian particles are used to depict the transport of contaminant. These particles can be sized to specific radii and for density to account for deposition. The trajectories for the Lagrangian particles are either interpolated using the finite element approximation functions or global interpolation functions. The particle trajectories are calculated in the global coordinate system. Distance of travel is determined by the time increment. This increment is calculated by limiting particle advection

to be no further than its neighboring element. Particulate diffusivities are determined by a Monte Carlo/random walk method [10, 11, 12].

Results

Figure 2 shows transient dispersion of PM_{10} and larger particles released from near ground level sources around buildings. The distance a particle travels is dependent on its aerodynamic diameter and the effectiveness of gravitational settling. As the flow slows and swirls in the proximity of buildings or natural obstructions, concentrations increase. Deposition of the entrained particles occurs by impact with surfaces and by settling. Entrained particles shown in Fig. 2 are being transported and deposited around several buildings typical of structures.

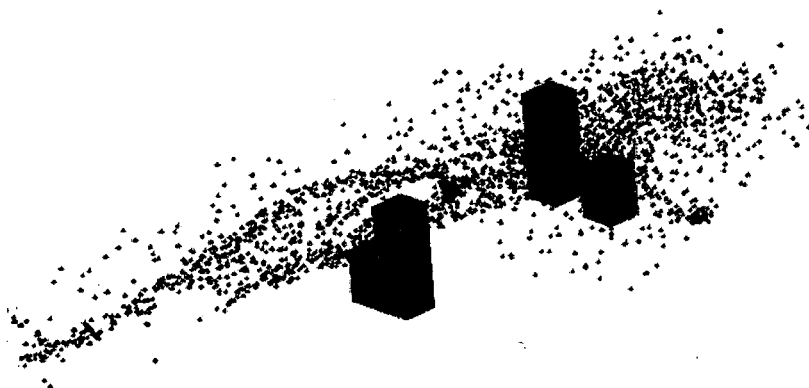


Figure 2: Transport and deposition of particles around buildings.

References

1. Li, J., Hon, Y. C., and Chen, C. S. (2002): Numerical comparisons of two meshless methods using radial basis functions, *Engineering Analysis with Boundary Elements*, Elsevier Science Ltd., 26, pp. 205-225.
2. Atluri, S. N., Kim, H. K., and Cho, J.Y. (1999): A critical assessment of the truly meshless local Petrov-Galerkin (MLPG), and local boundary integral equation (LBIE) methods, *Computational Mechanics*, 24, pp. 348-372.
3. Liu, G. R. (2002): *Mesh Free Methods: Moving Beyond the Finite Element Method*, CRC Press, Boca Raton, FL.
4. Mfree2d - <http://www.nus.edu.sg/ACES/software/meshless2D/webfiles/webpageMFree.htm>
5. Atluri, S. N. and Shen, S. (2002): *The Meshless Local Petrov Galerkin (MLPG) Method*, Tech Science Press, Encino, CA.
6. Kansa, E. J. (1990): Multiquatic – A scattered data approximation scheme with applications to computational fluid dynamics II, *Computers Math. Appl.*, 19, 8/9, pp. 147-161.
7. Powell, M. J. D. (1992): The theory of radial basis function approximation in 1990, in *Advances in Numerical Analysis*, Vol. II, W. Light (Ed.), Oxford Sci. Pub., Oxford, UK, pp. 105-210.
8. Pepper, D. W. and Carrington, D. B. (1999): Application of h-Adaptation for Environmental Fluid Flow and Species Transport, *Int. J. Num. Meth. Fluids*, 31, pp. 275-283.

9. Lee, R. L., Leone, J. M. Jr., and Gresho, P. M. (1983): Modified finite element model for application to terrain-induced mesoscale flows, *AMS 6th Symp. on Turbulence and Diffusion*, Boston, MA.
10. Carrington, D. B. and Pepper, D. W. (1998): Prediction of species transport in urban canyons using an h-adaptive finite element approach, *Development and Application of Computer Techniques to Environmental Studies*, Pepper, Brebbia, Zannetti, Computational Mechanics Publications, WIT Press, pp. 53-64.
11. Carrington, D. B. and D. W. Pepper (1999): A boundary element model for indoor air quality simulation, *Boundary Element Technology XIII*, C. S. Chen, C. A. Brebbia, and D. W. Pepper (Eds.), WIT Press, Southampton, UK, pp. 53-61.
12. Zannetti P. and R. Sire (1999): MONTECARLO-A New, fully-integrated PC software for the 3D simulation and visualization of air pollution dispersion using Monte Carlo Lagrangian particle (MCLP) techniques, *Conf. Air Pollution 99*, Stanford, CA.